A DIRECT DERIVATION OF TRANSFORMS FOR WAVE-DOMAIN ADAPTIVE FILTERING BASED ON CIRCULAR HARMONICS

Martin Schneider and Walter Kellermann

Multimedia Communications and Signal Processing*
University of Erlangen-Nuremberg
Cauerstr. 7, 91058 Erlangen, Germany
mail: {schneider,wk} @LNT.de

ABSTRACT

Wave-domain adaptive filtering (WDAF) is advantageous for modeling loudspeaker-enclosure-microphone systems with many loudspeakers and microphones (MIMO LEMS). The necessary transforms may be derived by considering free field propagation between loudspeaker and microphones first, followed by wave field analysis of the true and simulated microphone signals. However, transforms obtained following this strategy are not invertible when there are more loudspeakers than microphones. As invertibility of the transforms is required for many applications, this restricts the applicability of WDAF. In this paper we propose a strategy to describe the free field propagation directly in the wave domain, so that invertible transforms can be defined independently from the number of actually used microphones. With this strategy, transforms for a MIMO LEMS comprising a uniform circular microphone array and an arbitrary loudspeaker array are derived.

Index Terms— Adaptive filtering, multichannel, wave domain

Emerging techniques like wave field synthesis (WFS) or Higher-Order Ambisonics (HOA) aim at providing high-quality spatial reproduction of an acoustic scene. To facilitate new application fields or to improve the reproduction quality these reproduction systems may be complemented by a spatial recording system and adaptive filtering techniques. Prominent application examples are acoustic echo cancellation (AEC) or adaptive listening room equalization (LRE). However, the typically large number of reproduction channels for WFS or HOA makes adaptive filtering challenging due to computational and algorithmic reasons.

Wave-domain adaptive filtering (WDAF) was proposed for various adaptive filtering tasks in the context of massive multichannel reproduction systems [1, 2]. Using fundamental solutions of the wave-equation as basis functions for the wave-domain signal representations, WDAF enables the use of a physically motivated approximation of the MIMO LEMS, which allows to significantly reduce the computational effort for adaptive filtering [1]. In the following, we investigate the transformations of the loudspeaker signals and the microphone signals into the wave domain and refer to them as transforms T1 and T2, respectively, to indicate the sequence of processing. The wave-domain loudspeaker signal representation will be denoted as free-field description and the wave-domain microphone signal representation as measured wave field. Using the chosen basis functions, transform T2 simply describes the sound pressure measured by the microphones, while transform T1 describes the wave field, as it ideally would be produced by the loudspeaker array at the microphone array under free-field conditions. Consequently, transform T1 comprises two steps, the free-field propagation of the sound from the loudspeakers to the microphones and a transform of the resulting sound pressure to the wave-domain. Originally, it was proposed to model the free-field propagation as point-to-point propagation between all respective loudspeaker and the microphone positions. The signal representation obtained from this should then be transformed by transform T2 [1]. Considering the desired transforms, this strategy is the obvious choice, but it has some disadvantages. The most significant is that the number of linearly independent wave field components of the free-field description is limited by the number of microphones, which may be less than the number of loudspeakers. Thus, spatial information is lost and the original loudspeaker signals cannot be reconstructed from the free-field description. This precludes the use of such a transform for LRE and even AEC would suffer from the resulting lack of degrees of freedom in the wave-domain MIMO LEMS model. Here, we propose another strategy for defining the transform T1. To this end, we describe the free-field wave field as produced by the loudspeakers at the position of the microphone array directly in the wave domain. This has the advantage that the loudspeaker signal transform is independent of the actual number of microphones, while there are no disadvantages compared to the original approach. With this strategy, we derive transforms for an arbitrarily shaped loudspeaker array

*This work was supported by the Fraunhofer Institute for Digital Media Technology (IDMT) in Ilmenau, Germany.

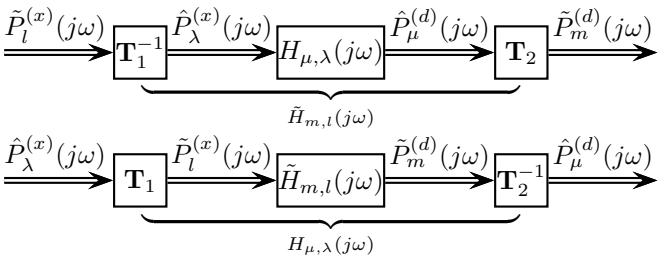

Fig. 1. Roles of the transforms and their inverses. Upper row: wave-domain representation of MIMO LEMS, lower row: point-to-point model with embedded wave-domain MIMO-LEMS.

and a circular microphone array whereby an optional cylindrical scatterer within the microphone array can be considered. Thus, we provide an explicit formulation of the transforms to the wave-domain, which was not included in [1] and [2] and generalize the transforms mentioned in [3], which are limited to concentrically located circular transducer arrays.

The paper is organized as follows: In Sec. 1 the MIMO LEMS model and its desired properties are discussed. In Sec. 2 the transforms are derived based on a continuous-frequency description. In Sec. 3 the derived transforms are formulated for discrete-time signal processing. Measurement results demonstrating the practical impact of the transforms are presented in Sec. 4 and conclusions are given in Sec. 5.

1. WAVE-DOMAIN MIMO LEMS MODEL

In this section the wave-domain MIMO LEMS model and its attractive properties are reviewed [3]. For the conventional point-to-point model, we consider the N_L spectra of the signals emitted by the loudspeakers $\hat{P}_\lambda^{(x)}(j\omega)$ ($\lambda = 0, \ldots, N_L - 1$) and the N_M spectra of the sound pressure signals $\hat{P}_\mu^{(d)}(j\omega)$ ($\mu = 0, \ldots, N_M - 1$) measured by the microphones and obtain

$$\hat{P}_\mu^{(d)}(j\omega) = \sum_{\lambda=0}^{N_L-1} \hat{P}_\lambda^{(x)}(j\omega) H_{\mu,\lambda}(j\omega), \qquad (1)$$

to model the MIMO LEMS by $N_M \times N_L$ frequency responses $H_{\mu,\lambda}(j\omega)$, where λ and μ denote the loudspeaker and microphone indices, respectively. Equivalently, we may describe a wave-domain model using the free-field description $\tilde{P}_l^{(x)}(j\omega)$ obtained from transform T1 and the measured wave field $\tilde{P}_m^{(d)}(j\omega)$ as the output of transform T2:

$$\tilde{P}_m^{(d)}(j\omega) = \sum_{l=-N_L/2+1}^{N_L/2} \tilde{H}_{m,l}(j\omega) \tilde{P}_l^{(x)}(j\omega), \qquad (2)$$

where l and m are indexing the modes in $\tilde{P}_l^{(x)}(j\omega)$ and $\tilde{P}_m^{(d)}(j\omega)$, respectively, and $\tilde{H}_{m,l}(j\omega)$ models their couplings. The roles of the transforms for modeling the MIMO LEMS in the conventional or in the wave domain are depicted in Fig. 1. Although, (1) and (2) are equivalent in their ability to model the MIMO LEMS, $H_{\mu,\lambda}(j\omega)$ and $\tilde{H}_{m,l}(j\omega)$ differ

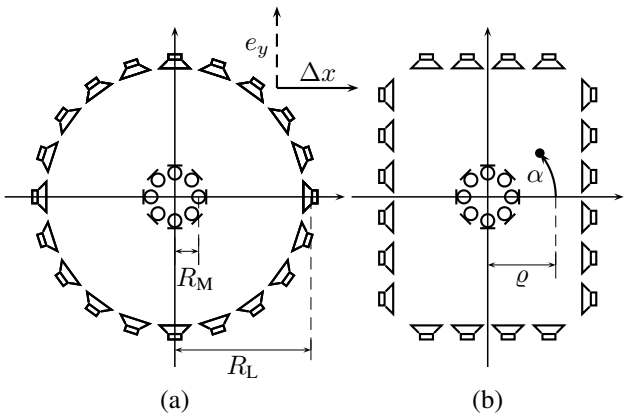

Fig. 2. Exemplary loudspeaker and microphone setups of the modeled MIMO LEMS

significantly in their properties. For illustration, we measured all frequency responses $H_{\mu,\lambda}(j\omega)$ between the $N_L = 48$ loudspeakers and the $N_M = 10$ microphones of a MIMO LEMS in a room with a reverberation time of $T_{60} \approx 0.3$s. The uniform circular loudspeaker and microphone arrays where concentrically located, as shown in Fig. 2(a), with radii $R_L = 1.5$m and $R_M = 0.05$m. Using the transforms as derived below in Sec. 2, $\tilde{H}_{m,l}(j\omega)$ was determined from $H_{\mu,\lambda}(j\omega)$. Their magnitudes are shown in Fig. 3 for three different frequencies ω. It can be clearly seen that while all the loudspeaker-microphone couplings are approximately equally strong, in the wave domain, some couplings in the vicinity of the diagonal $l = m$ are significantly more important than the rest. This diagonal dominance in $|\tilde{H}_{m,l}(j\omega)|$ leads to a decisive algorithmic and computational advantage over conventional point-to-point models for adaptive filtering tasks [1, 2, 3], e. g., the possibility to model the MIMO LEMS by only its dominant wave-domain couplings.

2. DERIVATION OF THE TRANSFORMS

In this section, the actual wave-domain transforms T1 and T2 are derived, generalizing the transforms used in [3]. As, for WDAF, the MIMO LEMS is considered as a spatially sampled wave field, the transducer positions, i. e., the sampling positions have to be known exactly. This work is concerned with transducer arrays located in a plane, where we assume the microphone array to be a uniform circular array while the loudspeaker array may have an arbitrary shape. Examples of such setups are shown in Fig. 2. Within this work, the loudspeaker positions are given in polar coordinates by $\vec{l}_\lambda = (\alpha_\lambda, \varrho_\lambda)^T$. The microphone array consists of equispaced microphones on a circle with radius R_M, with the positions given by

$$\vec{m}_\mu = \left(\alpha_\mu = \mu \cdot \frac{2\pi}{N_M}, \varrho_\mu = R_M\right)^T. \qquad (3)$$

Considering a circular microphone array, a natural choice for the wave-domain basis functions are the so-called circular

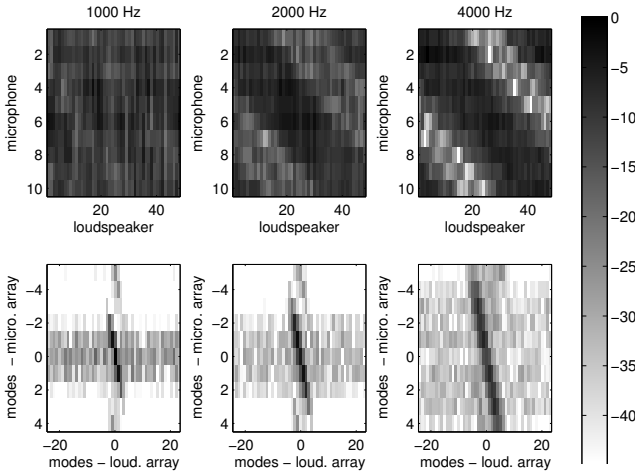

Fig. 3. Logarithmic magnitudes of $H_{\mu,\lambda}(j\omega)$ and $\tilde{H}_{m,l}(j\omega)$ in dB with $\mu = 0, \ldots, N_M - 1$, $\lambda = 0, \ldots, N_L - 1$, and $m = -4, \ldots, 5$, $l = -23, \ldots, 24$, for different frequencies $\omega = 2\pi f$, $f = 1\,\text{kHz}, 2\,\text{kHz}, 4\,\text{kHz}$ normalized to the maximum of all subfigures in each row.

harmonics [4], while plane waves would be more suitable for linear array geometries. Thus we describe the spectrum of the sound pressure $P(\alpha, \varrho, j\omega)$ at any point $\vec{x} = (\alpha, \varrho)^T$ by a sum of circular harmonics

$$P(\alpha, \varrho, j\omega) = \sum_{m=-\infty}^{\infty} \Big(\tilde{P}_m^{(1)}(j\omega) \mathcal{H}_m^{(1)}(k\varrho) + \tilde{P}_m^{(2)}(j\omega) \mathcal{H}_m^{(2)}(k\varrho) \Big) e^{jm\alpha}, \quad (4)$$

where $\mathcal{H}_m^{(1)}(x)$ and $\mathcal{H}_m^{(2)}(x)$ are m-th order Hankel functions of the first and second kind, respectively. The imaginary unit is denoted by j and $k = \omega/c$ is the wave number with the angular frequency ω and the speed of sound c. Assuming no acoustic sources within the microphone array, it is sufficient to consider the superposition of incoming waves $\tilde{P}_m^{(1)}(j\omega)$ and outgoing waves $\tilde{P}_m^{(2)}(j\omega)$ and describe $\tilde{P}_m^{(d)}(j\omega)$ by

$$\tilde{P}_m^{(d)}(j\omega) B_m(k\varrho) = \tilde{P}_m^{(1)}(j\omega) \mathcal{H}_m^{(1)}(k\varrho) + \tilde{P}_m^{(2)}(j\omega) \mathcal{H}_m^{(2)}(k\varrho), \quad (5)$$

where $B_m(kR_M) = \mathcal{J}_m(kR_M)$ in the free field and

$$B_m(kR_M) = \mathcal{J}_m(kR_M) - \frac{\mathcal{J}_m'(kR_M)\mathcal{H}_m^{(1)}(kR_M)}{\mathcal{H}_m'(kR_M)} \quad (6)$$

if there is a cylindrical scatterer within the microphone array. Here, $\mathcal{J}_m(x)$ is the m-th order Bessel function and $\mathcal{J}_m'(x)$ and $\mathcal{H}_m'(x)$ are the derivatives of $\mathcal{J}_m(x)$ and $\mathcal{H}_m^{(1)}(x)$ with respect to x, respectively [5]. This set of basis functions is similar to those used in [6].

2.1. Transform T2

Transform T2 is used to obtain the wave field represented by the actual microphone signals. Using (4) to describe the sound field in the vicinity of the microphone array, we can obtain $\tilde{P}_m^{(d)}(j\omega)$ by a Fourier series expansion:

$$B_m(kR_M)\, \tilde{P}_m^{(d)}(j\omega) = \frac{1}{2\pi} \int_0^{2\pi} P(\alpha, R_M, j\omega) e^{-jm\alpha} d\alpha. \quad (7)$$

Since we can only use a finite number of microphones in practice, we sample the wave field at discrete positions and approximate the integral in (7) by a sum to obtain

$$\tilde{P}_m^{(d)}(j\omega) := \frac{1}{N_M B_m(kR_M)} \sum_{\mu=0}^{N_M-1} \hat{P}_\mu^{(d)}(j\omega) e^{-jm\alpha_\mu}. \quad (8)$$

Due to the finite sum in (8), there are only N_M non-redundant modes observable, so we consider only the mode orders $m = -(N_M/2 - 1), \ldots, N_M/2$.

From (8), we may directly derive the inverse of transform T2, which is given by

$$\hat{P}_\mu^{(d)}(j\omega) = \sum_{m=-N_M/2+1}^{N_M/2} B_m(kR_M)\, \tilde{P}_m^{(d)}(j\omega) e^{jm\alpha_\mu}. \quad (9)$$

2.2. Transform T1

In this section we derive the transform T1 which is used to describe the wave field emitted by the loudspeakers as it would appear at the microphone array under free-field conditions. As we only consider a two-dimensional wave field, while the actual wave propagation between the loudspeakers and the microphone array is three-dimensional in reality, such a description only represents an approximation. Assuming a large minimum loudspeaker-microphone distance ($R_M \ll \min\{\varrho_\lambda\}$) and considering only wavelengths larger than R_M, we describe all loudspeaker contributions at the position of the microphone array, i. e., the origin of the coordinate system, as plane waves [7]. As the true loudspeakers are better described as point-like sources than as plane sources, we describe the resulting attenuation and the delay for the wave propagation from the individual loudspeakers to the origin of the microphone array by the three-dimensional Green's function [8]

$$G(\vec{0}|\vec{l}_\lambda, j\omega) = \frac{e^{-j\varrho_\lambda k}}{\varrho_\lambda}. \quad (10)$$

From (10) we may derive an intermediate transform providing an approximate plane wave decomposition of the loudspeaker contributions at the origin:

$$\tilde{P}_\lambda^{(p)}(j\omega) \approx \hat{P}_\lambda^{(x)}(j\omega) G(\vec{0}|\vec{l}_\lambda, j\omega), \quad (11)$$

where $\tilde{P}_\lambda^{(p)}(j\omega)$ describes the spectrum of a plane wave with the incidence angle α_λ. However, as we use circular harmonics as basis functions, we have to transform $\tilde{P}_\lambda^{(p)}(j\omega)$ again. As $R_M \ll \min\{\varrho_\lambda\}$, we may also assume the attenuation through the propagation along the microphone array as being negligible compared to (10). The sound pressure resulting from the superposition of all $\tilde{P}_\lambda^{(p)}(j\omega)$ is given by

$$P(\alpha, \varrho, j\omega) = \sum_{\lambda=0}^{N_L-1} \tilde{P}_\lambda^{(p)}(j\omega) e^{j\varrho\cos(\alpha-\alpha_\lambda)k}. \quad (12)$$

According to [3] we may use the Jacobi-Anger expansion to transform (12) using (7). The frequency response resulting from a possible scatterer inside the circular microphone array is already equalized by (8), so we may disregard a possible scatterer for the derivation of transform T1. With this assumption and by substituting m by l relative to (8), we obtain

$$\tilde{P}_l^{(x)}(j\omega) = j^l \sum_{\lambda=0}^{N_L-1} \tilde{P}_\lambda^{(p)}(j\omega) e^{-jl\alpha_\lambda}. \quad (13)$$

As for the microphones in (8), we account for the limited spatial resolution of the loudspeaker array and limit the consideration to N_L non-redundant components $l = -(N_L/2 - 1), \ldots, N_L/2$. From (11) and (13), we obtain the explicit definition of transform T1

$$\tilde{P}_l^{(x)}(j\omega) := j^l \sum_{\lambda=0}^{N_L-1} \hat{P}_\lambda^{(x)}(j\omega) \frac{e^{-j\varrho_\lambda k}}{\varrho_\lambda} e^{-jl\alpha_\lambda}. \quad (14)$$

The inverse of T1 may also be derived straightforwardly in two stages. From (13) we may directly derive

$$\tilde{P}_\lambda^{(p)}(j\omega) = \frac{1}{N_L} \sum_{l=-N_L/2+1}^{N_L/2} \tilde{P}_l^{(x)}(j\omega) j^{-l} e^{jl\alpha_\lambda}. \quad (15)$$

As the $e^{-j\varrho_\lambda k}$ term in (10) describes a delay, an inverse of (11) would be non-causal, requiring a delay by $\max\{\varrho_\lambda\}/c$ for realizability. Assuming furthermore that (11) holds for an equation rather than an approximation, leads to

$$\hat{P}_\lambda^{(x)}(j\omega) := \tilde{P}_\lambda^{(p)}(j\omega) \varrho_\lambda e^{j(\varrho_\lambda - \max\{\varrho_\lambda\})k}, \quad (16)$$

so that the inverse of transform T1 is given by (15) and (16).

3. DISCRETE-TIME REPRESENTATIONS OF THE TRANSFORMS

In this section, discrete-time or DFT-domain-compatible representations of the derived transforms are presented. Considering (8) we can see that transform T2 may be realized in two steps: A DFT with respect to the microphone indices and the inverse of $B_m(kR_M)$. The first step is easy to realize because there is no frequency-dependency to be considered. Consequently, this part of the transform remains identical, independently of any temporal transform. The inverse of $B_m(kR_M)$ has only a frequency-dependency but no spatial dependency. Thus, filter-design methods may be used to determine a suitable FIR or IIR filter for each m separately. However, when there is no scatterer within the microphone array $B_m(kR_M)$ exhibits zeros rendering the design of a perfect inverse impossible. To circumvent this problem we use $B_m(kR_M)\tilde{P}_m^{(d)}(j\omega)$ instead of $\tilde{P}_m^{(d)}(j\omega)$ as representation for the measured wave field. By doing so, $B_m(kR_M)$ (and not its inverse) is modeled implicitly in the MIMO LEMS model, rendering a filter design for transform T2 unnecessary. For acoustic echo cancellation (AEC) this is preferable because it simplifies the realization of the transforms without any cost [3]. For listening room equalization (LRE) all signal representations remain consistent, but it has to be considered that the minimized error signal for the measured wave field does no longer directly describe the distortion of the reproduced wave field apart from the microphone positions, but a frequency-dependent weighting of this error is introduced. For the inverse of T2, the spatial transform follows the filtering of the individual wave-domain signals, where the filter design according to $B_m(kR_M)$ is less challenging than for its inverse. Again, when using $B_m(kR_M)\tilde{P}_m^{(d)}(j\omega)$ as representation for the measured wave field, no filter design is required.

The description of transform T1 in two steps allows a realization procedure similar to transform T2. The realization of (11) is straightforward, as it can be accomplished by fractional delay filters [9], while (13) can be directly applied due to its frequency-independence. The same holds for (16) and (15), respectively.

To give an example of the realized transforms we use $B_m(kR_M)\tilde{P}_m^{(d)}(j\omega)$ for transform T2. Consequently, (8) and (9) may be directly used, i. e., represented by a $N_M \times N_M$ MIMO FIR-filter structure describing weighted Kronecker deltas. For transform T1, we have to define the discrete-time impulse responses

$$h_{l,\lambda}^{(\mathrm{T1})}(n) = j^l \frac{h_d(n, \varrho_\lambda f_s/c)}{\varrho_\lambda} e^{-jl\alpha_\lambda}, \quad (17)$$

which are used for computing the contribution of the discrete-time loudspeaker signal λ to the wave field component l in the free-field description according to (14). Here, f_s is the sampling frequency and

$$h_d(n, d) = \begin{cases} \frac{\sin(\pi(n-d-(L_T-1)/2))}{\pi(n-d-(L_T-1)/2)} & \text{for } 0 \le n < L_T, \\ 0 & \text{elsewhere} \end{cases} \quad (18)$$

is an FIR filter with the odd length L_T according to [9] describing the non-integer delay d. For the inverse of T1, we may write in the same way

$$h_{\lambda,l}^{(\mathrm{T1i})}(n) = j^{-l} h_d(n, (\max\{\varrho_\lambda\} - \varrho_\lambda) f_s/c) \varrho_\lambda \frac{e^{jl\alpha_\lambda}}{N_L}. \quad (19)$$

4. VALIDATION OF THE DERIVED TRANSFORMS

In this section the derived wave-domain transforms are validated with measured impulse responses. For the evaluation, we consider the total energy of the mode couplings by

$$E_{m,l} = \frac{1}{2\pi} \int_0^{\omega_{\max}} |\tilde{H}_{m,l}(j\omega)|^2 d\omega, \quad (20)$$

where $\omega_{\max} = 2\pi 4000$Hz is the maximum considered frequency. For the MIMO LEMS the concentric array setup as described in Sec. 1 was considered. In contrast to Sec. 1

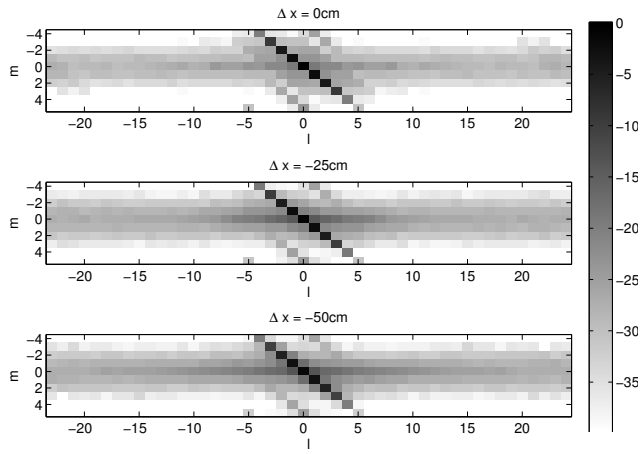

Fig. 4. Total energy $E_{m,l}$ of the mode couplings for different array setups in dB with respect to $\max\{E_{m,l}\}$. The loudspeaker array is shifted by Δx on the x-axis.

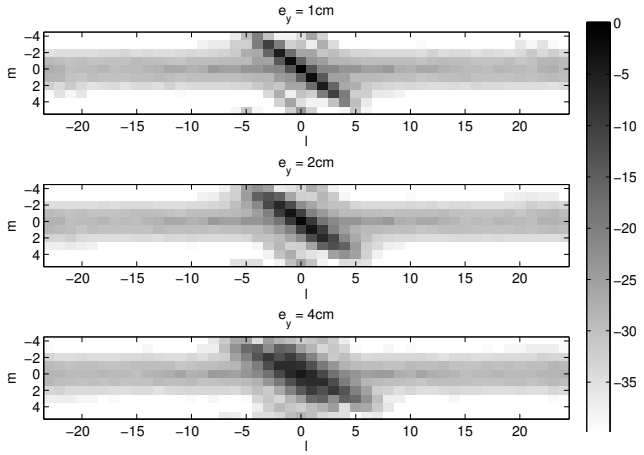

Fig. 5. Total energy $E_{m,l}$ of the mode couplings for accurate array positioning in dB with respect to $\max\{E_{m,l}\}$. A deviation by e_y along the y-axis was introduced.

the position of the circular loudspeaker array was shifted as stated, or incorrect information about the array position was used for the derivation of the transforms. For the inverse of transform T1 and transform T2, we used the example from Sec. 3 with $L_T = 151$ and $f_s = 8000$Hz. In Fig. 4, $E_{m,l}$ is shown for different array setups. There, the loudspeaker array was shifted by Δx on the x-axis to show the suitability of the transforms for differently located loudspeaker arrays. For the array setups shifted by $\Delta x = 0, -25$, and -50cm, respectively, the diagonal couplings cover $89.7\%, 80.8\%$, and 75.6% of the total energy of all couplings, respectively. Since the diagonal-dominant structure may be preserved, we can state that the presented transforms are suitable for different array setups. However, the small loudspeaker-microphone distances for larger Δx degrade the diagonal dominance, which is not surprising, because we required a large loudspeaker-microphone distance with $R_M \ll \min\{\varrho_\lambda\}$ in the derivation. This result may be generalized to other loudspeaker array geometries.

For the results shown in Fig. 4, perfect knowledge about the true array positions was assumed. In practice, positioning errors must be expected. To evaluate the robustness of a WDAF system against mispositioned arrays, we determined $E_{m,l}$ for wave-domain transforms based on inaccurate knowledge about loudspeaker array position, where we introduced an error e_y in y-direction. In Fig. 5 we can see that an error e_y of 1cm does not destroy the desired diagonal dominance and an error of e_y of 2cm might be marginally acceptable. For an error e_y of 4cm, we can see that the desired properties of the wave-domain representation are seriously impaired. The diagonal couplings cover 81.2%, 60.9%, and 24.7% of the total coupling energy for $e_y = 1, 2$, and 4cm, respectively.

5. CONCLUSIONS

In this paper generic transforms to and from the wave domain for a MIMO LEMS with a circular microphone array and an arbitrarily shaped loudspeaker array were discussed. The realization of those transforms with discrete-time systems was also presented. Measurement results show that these transforms are suitable for practically relevant array setups, whereby an array mispositioning up to several centimeters appears to be acceptable. A future research goal is the extention of this strategy to other microphone array geometries.

6. REFERENCES

[1] H. Buchner, S. Spors, and W. Kellermann, "Wave-domain adaptive filtering: acoustic echo cancellation for full-duplex systems based on wave-field synthesis," in *Proc. Int. Conf. Acoust., Speech, Signal Process. (ICASSP)*, May 2004, vol. 4, pp. IV–117 – IV–120.

[2] S. Spors, H. Buchner, and R. Rabenstein, "A novel approach to active listening room compensation for wave field synthesis using wave-domain adaptive filtering," in *Proc. Int. Conf. Acoust., Speech, Signal Process. (ICASSP)*, May 2004, vol. 4, pp. IV–29 – IV–32.

[3] M. Schneider and W. Kellermann, "A wave-domain model for acoustic MIMO systems with reduced complexity," in *Proc. Joint Workshop on Hands-free Speech Communication and Microphone Arrays (HSCMA)*, Edinburgh, UK, May 2011.

[4] S. Spors, H. Buchner, R. Rabenstein, and W. Herbordt, "Active listening room compensation for massive multichannel sound reproduction systems using wave-domain adaptive filtering," *J. Acoust. Soc. Am.*, vol. 122, no. 1, pp. 354 – 369, Jul. 2007.

[5] H. Teutsch, *Modal Array Signal Processing: Principles and Applications of Acoustic Wavefield Decomposition*, Springer, Berlin, 2007.

[6] T. Betlehem and T.D. Abhayapala, "Theory and design of sound field reproduction in reverberant rooms," *J. Acoust. Soc. Am.*, vol. 117, no. 4, pp. 2100 – 2111, April 2005.

[7] C.A. Balanis, *Antenna Theory*, Wiley, New York, 1997.

[8] P. Morse and H. Feshbach, *Methods of Theoretical Physics*, Mc Graw - Hill, New York, 1953.

[9] T. Laakso, V. Välimäki, M. Karjalainen, and U. Laine, "Splitting the unit delay," *IEEE Signal Process. Mag.*, pp. 30–60, Jan. 1996.